

## Čerenkov difference frequency generation in a two-dimensional nonlinear photonic crystal

C. D. Chen, X. P. Hu, Y. L. Xu, P. Xu, G. Zhao, and S. N. Zhu

Citation: [Applied Physics Letters](#) **101**, 071113 (2012); doi: 10.1063/1.4746408

View online: <http://dx.doi.org/10.1063/1.4746408>

View Table of Contents: <http://scitation.aip.org/content/aip/journal/apl/101/7?ver=pdfcov>

Published by the [AIP Publishing](#)

---

### Articles you may be interested in

[Čerenkov third-harmonic generation in  \$\chi\(2\)\$  nonlinear photonic crystal](#)

Appl. Phys. Lett. **98**, 241114 (2011); 10.1063/1.3602312

[Directional dependence of the second harmonic response in two-dimensional nonlinear photonic crystals](#)

Appl. Phys. Lett. **96**, 261111 (2010); 10.1063/1.3459975

[All-optical switching of defect mode in two-dimensional nonlinear organic photonic crystals](#)

Appl. Phys. Lett. **87**, 231111 (2005); 10.1063/1.2140092

[Optical amplification in two-dimensional photonic crystals](#)

Appl. Phys. Lett. **86**, 091111 (2005); 10.1063/1.1879094

[Second-harmonic green generation from two-dimensional  \$\chi\(2\)\$  nonlinear photonic crystal with orthorhombic lattice structure](#)

Appl. Phys. Lett. **83**, 3447 (2003); 10.1063/1.1622786

---

Frustrated by old technology?      Is your AFM dead and can't be repaired?      Sick of bad customer support?

**It is time to upgrade your AFM**  
Minimum \$20,000 trade-in discount  
for purchases before August 31st

**Asylum Research is today's  
technology leader in AFM**

dropmyoldAFM@oxinst.com

**OXFORD**  
INSTRUMENTS  
*The Business of Science®*

# Čerenkov difference frequency generation in a two-dimensional nonlinear photonic crystal

C. D. Chen,<sup>1</sup> X. P. Hu,<sup>1,a)</sup> Y. L. Xu,<sup>2</sup> P. Xu,<sup>1</sup> G. Zhao,<sup>2</sup> and S. N. Zhu<sup>1</sup>

<sup>1</sup>National Laboratory of Solid State Microstructures and School of Physics, Nanjing University, Nanjing 210093, China

<sup>2</sup>College of Engineering and Applied Sciences, Nanjing University, Nanjing 210093, China

(Received 4 July 2012; accepted 2 August 2012; published online 14 August 2012)

We present experimental realization of Čerenkov difference frequency generation (CDFG) in a 2-dimensional rectangular periodically poled LiTaO<sub>3</sub>. The backward reciprocal vector of the nonlinear photonic crystal accelerates the phase velocity of the nonlinear polarization wave so as to exceed the phase speed limit of achieving Čerenkov down-conversions in this normal dispersion medium. Some characteristics of CDFG, such as radiation angles, pumping power, and pulse temporal overlapping dependences were discussed. The experimental results matched well with theoretical predictions. © 2012 American Institute of Physics. [<http://dx.doi.org/10.1063/1.4746408>]

The conventional Čerenkov radiation in particle physics is due to a charged particle moving faster than the velocity of the light in medium.<sup>1</sup> In nonlinear optics, when two laser beams with frequencies  $\omega_1$  and  $\omega_2$  are focused into a nonlinear crystal, 2nd-order nonlinear polarization waves (NPW) including  $2\omega_1$ ,  $2\omega_2$ ,  $\omega_1 + \omega_2$ , and  $\omega_1 - \omega_2$  are generated. By analogy with the conventional Čerenkov radiation, each of these nonlinear polarizations may be considered to be a source for the generation of nonlinear Čerenkov radiation (NCR). The earliest observation of NCR was realized in a ZnS planar waveguide reported by Tien *et al.*<sup>2</sup> Since then, varieties of studies of Čerenkov second harmonic generation (CSHG)<sup>3,4</sup> and Čerenkov sum-frequency generation (CSFG)<sup>5-7</sup> realized in optical waveguides had been reported. More recently, by use of ultra-short laser light sources, it was found that NCR could be highly enhanced due to the existence of domain wall in bulk nonlinear photonic crystals (NPC).<sup>8</sup> Besides CSHG (Refs. 9-14) and CSFG,<sup>15</sup> third-harmonic<sup>16,17</sup> or much higher-order<sup>18</sup> Čerenkov radiations could also be generated via cascaded 2nd-order nonlinear processes.

However, all the Čerenkov radiations mentioned above, whether in optical waveguides or in bulk crystals, were Čerenkov up-conversions, which made use of the terms  $2\omega_1$ ,  $2\omega_2$ , or  $\omega_1 + \omega_2$ . As is well known, the realization of NCR should satisfy an important prerequisite: the phase velocity of NPW should be faster than that of the harmonics. In a normal dispersion medium, such phase velocity condition is naturally satisfied, so Čerenkov up-conversions are relatively easy to be achieved. But for Čerenkov down-conversions, the phase velocity of NPW  $\omega_1 - \omega_2$  can be expressed as

$$v_p = \omega_3 / \left( \frac{\omega_1}{v_1} - \frac{\omega_2}{v_2} \right), \quad (1)$$

where  $\omega_3$  is the difference frequency signal,  $v_1$ ,  $v_2$  are the phase velocities of  $\omega_1$  and  $\omega_2$ , respectively. The phase velocity of the NPW ( $v_p$ ) is generally smaller than that of harmonic ( $v'$ ), so Čerenkov difference frequency generation

(CDFG) cannot be realized. In the previous works, we have reported that in dielectric waveguides with modulated 2nd-order nonlinearity ( $\chi^{(2)}$ ), the reciprocal vectors provided by the structure can modulate the phase velocity of NPW.<sup>19,20</sup> The phase velocity could be decreased by the forward reciprocal vectors while be accelerated by the backward ones. In this letter, we designed a 2D rectangular periodically-poled LiTaO<sub>3</sub> (PPLT) crystal, which not only utilized the domain walls but also introduced  $\chi^{(2)}$  modulations along the propagation direction of NPW  $\omega_1 - \omega_2$ , then  $v_p$  is modulated into

$$v_p = \omega_3 / \left( \frac{\omega_1}{v_1} - \frac{\omega_2}{v_2} - |\vec{G}| \right), \quad (2)$$

where  $\vec{G}$  is the reciprocal vector of PPLT. So with a proper  $\vec{G}$ , the phase speed limit may be broken, i.e.,  $v_p > v'$ , thus, CDFG process can be realized.

The layout of the experiment setup is depicted in Fig. 1(a). The fundamental source is a laser with a repetition rate of 10 Hz and delivers  $\sim 20$  ps pulses. There are two output ports: Port 1 delivers y-polarized 532-nm green light and Port 2 delivers z-polarized 1064-nm near infrared.  $M_1$  and  $M_2$  are mirrors coated for high reflectance ( $R > 99.9\%$  at  $45^\circ$ ) at both 532 nm and 1064 nm.  $W_1$  is a half-wave plate of 532 nm. In order to ensure the two pulses to get a good temporal overlapping, a prism  $P_1$  together with a translation stage is used to construct a simple delay line. The two incident beams are focused into the crystal along x-axis using a lens  $F_1$  with a focal length of 300 mm. Fig. 1(b) shows the simple schematic experimental diagram. The sample used in the experiment is a z-cut 2D rectangular PPLT with the dimension of 0.5 mm (x)  $\times$  8 mm (y)  $\times$  0.5 mm (z). To satisfy the phase velocity prerequisite for achieving CDFG of 532 nm and 1064 nm, we set the domain period of the sample to be  $\Lambda = 5.5 \mu\text{m}$ . A screen for projecting the radiations is placed behind the end facet of the nonlinear crystal.

In the experiment, we first opened port 2 and just allowed 1064 nm to be focused into the sample. The energy of 1064 nm was set to be about 0.25 mJ. As shown in Fig. 2(a), one could observe two green spots on the screen, which were both common CSHG radiations from the 2D

<sup>a)</sup>Author to whom correspondence should be addressed. Electronic mail: xphu@nju.edu.cn.

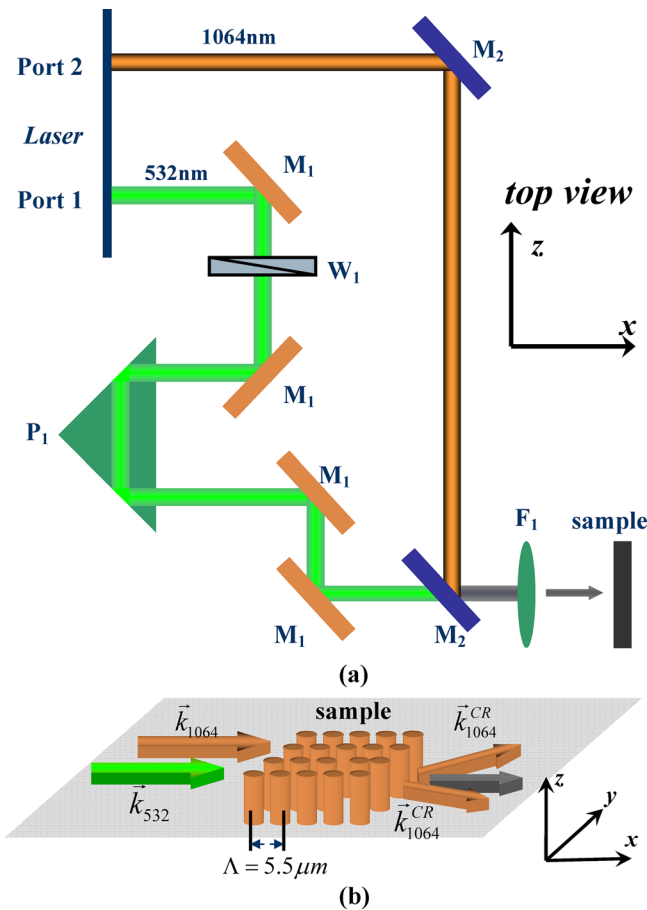


FIG. 1. The simple layout of the experimental setup from the top view.  $M_1$ : 45°-HR mirror at 532 nm,  $M_2$ : 45°-HR mirror at 1064 nm,  $W_1$ : half-wave plate of 532 nm,  $P_1$ : prism,  $F_1$ : lens with focal length of 300 mm (a). The schematic diagram of our experiment, the sample with the dimension of 0.5 mm ( $x$ )  $\times$  8 mm ( $y$ )  $\times$  0.5 mm ( $z$ ), is a  $z$ -cut 2D rectangular PPLT with a period of 5.5  $\mu\text{m}$  (b).

nonlinear photonic crystal. By measuring the Čerenkov radiation angles and taking the reciprocal vectors of the structure into consideration, we found that spot ② was a direct CSHG radiation with no reciprocal involved; while for spot ①, it was induced by a CSHG process with the 1st-order backward reciprocal vector participated, and in this case, the phase velocity of nonlinear polarization wave was equivalently increased, thus spot ① had a larger radiation angle than that of spot ②. The related phase-matching diagrams were shown on the right of each spot (Figs. 2(b) and 2(c)).

Substantively, we opened port 1 and mixed the two beams into the crystal. The energy of 532 nm and 1064 nm were set to be about 0.68 mJ and 0.4 mJ, respectively. In order to access the largest nonlinear coefficient  $d_{33}$ , the polarization of 532 nm was changed to  $z$ -direction which was the same as that of 1064 nm. When the prism was adjusted to an optimal position for the largest temporal overlapping of the two pulses, we can find another green spot ③ located between spots ① and ②, as shown in Fig. 3(a). According to our analysis, spot ③ resulted from the CDFG process cascaded with a CSHG process. Fig. 3(b) shows the phase-matching diagram of CDFG and it follows:

$$|\vec{k}_{532} - \vec{k}_{1064} - \vec{G}| = |\vec{k}_{1064}| \cos \theta_c^{DFG}, \quad (3)$$

in which  $\vec{k}_{532}$ ,  $\vec{k}_{1064}$  represent the wave-vectors of 532 nm and 1064 nm in the crystal, respectively,  $\vec{G} = \frac{2\pi}{\Lambda} \vec{x}$  is the 1st-order reciprocal vector,  $\theta_c^{DFG}$  is the radiation angle of CDFG. While the phase-matching diagram of the cascading CSHG process is shown in Fig. 3(c) and it follows:

$$|\vec{k}_{1064} + \vec{k}_{1064} \cos \theta_c^{DFG}| = |\vec{k}_{532}| \cos \theta_c'', \quad (4)$$

in which  $\theta_c''$  is the radiation angle. The generated signal at 1064 nm is invisible, however, the cascaded CSHG process

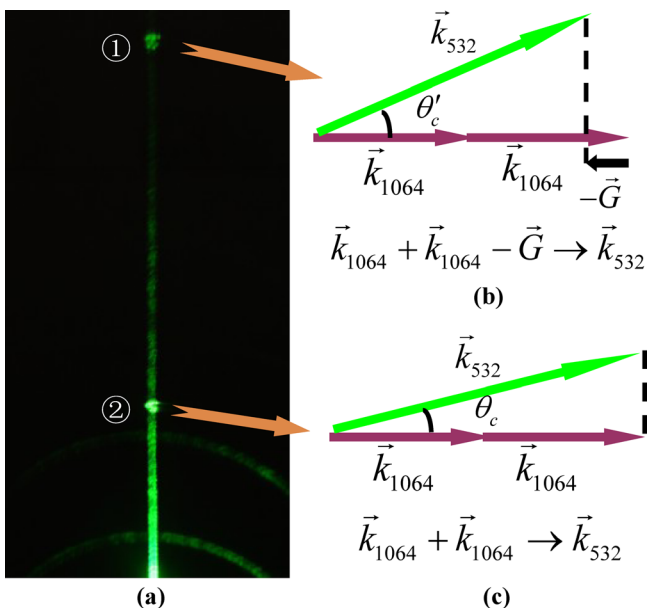


FIG. 2. The radiations projected on the screen when only 1064 nm was focused into the crystal (a). The phase-matching geometry of spot ① (b). The phase-matching geometry of spot ② (c).

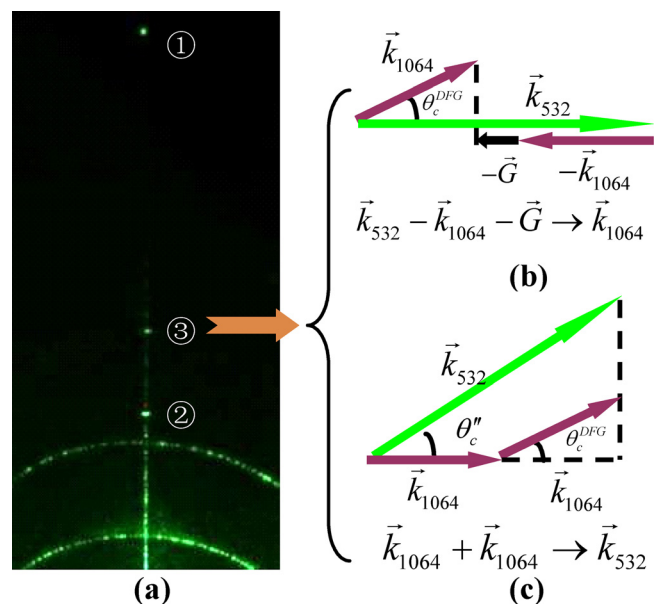


FIG. 3. The radiations projected on the screen when 1064 nm and 532 nm were mixed into the crystal together (a). The phase-matching geometry of the CDFG process (b). The phase-matching geometry of the cascaded CSHG process (c).

TABLE I. The theoretical ( $\theta_T$ ) and experimental ( $\theta_E$ ) emission angles of all the radiations (out of the crystal), including the common CSHG process (spots ① and ②), the CDFG process (the position of the near-infrared CDFG point was determined using a near-infrared fiber optical spectrometer), and the cascaded CSHG process (spot ③).

Type	Common CSHG		Cascaded CSHG	CDFG
Reciprocal vector involved	0	$-\vec{G}$	0	$-\vec{G}$
$\theta_T$	32.9°	56.8°	40.3°	29.6°
$\theta_E$	33.4°	57.7°	40.1°	29.2°

transformed the CDFG signal into a visible signal, which was spot ③ in the experiment. Such a visible signal reflects some characteristics of CDFG, which can offer us a relatively easy scheme for studying CDFG. We measured each Čerenkov angle as shown in Table I, including the common CSHG processes (spots ① and ②), the CDFG process and its cascaded CSHG process (spot ③). Table I also illustrated the calculated radiation angles out of the PPLT crystal, which matched well with the experimental values.

Theoretically, the CDFG intensity can be expressed as

$$I_{1064}^{CR} \propto d_{eff1}^2 \cdot I_{532} \cdot I_{1064} \cdot \int [f_{532}(t + \tau) \cdot f_{1064}(t)]^2 dt, \quad (5)$$

in which  $d_{eff1}$  is the effective nonlinear coefficient of the CDFG process,  $I_{1064}$  and  $I_{532}$  are the intensity of the input 1064 nm and 532 nm, respectively;  $f_{532}(t + \tau)$  and  $f_{1064}(t)$  represent the pulse profile of the input 532 nm and 1064 nm beams, respectively;  $\tau$  is the time delay between the two pulses. As for the cascaded CSHG process, the intensity of spot ③ can be written as  $I_3 \propto d_{eff2}^2 \cdot I_{1064} \cdot I_{1064}^{CR}$ , where  $d_{eff2}$  is the effective nonlinear coefficient of the cascaded CSHG process. Under an undepleted approximation of the pump at 1064 nm, we can get that the intensity of spot ③ is  $I_3 \propto I_{1064}^{CR} \propto \gamma I_{532}$ , in which  $\gamma = \int [f_{532}(t + \tau) \cdot f_{1064}(t)]^2 dt$  is the temporal overlapping of the two pulses. Keeping the power intensity of 1064 nm at 0.4 mJ and remaining the delay line in the optional position, we regulated the power intensity  $I_{532}$ , and the intensity tuning curve of spot ③ was

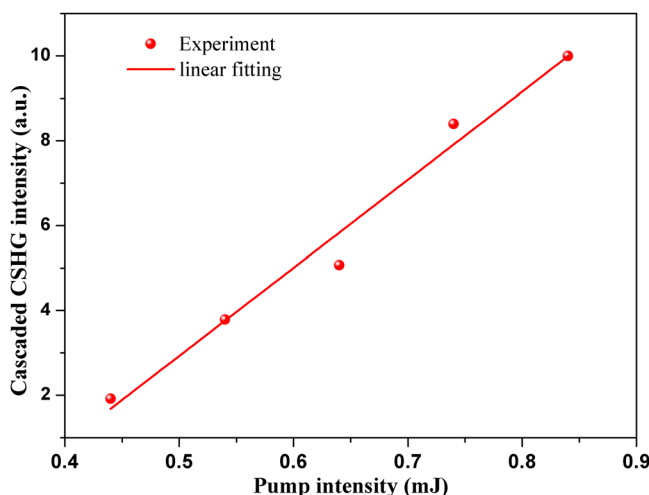
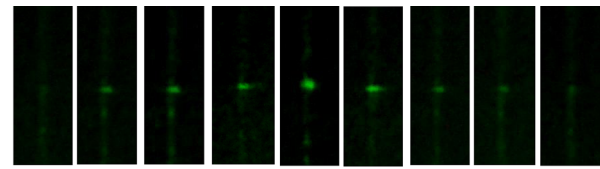
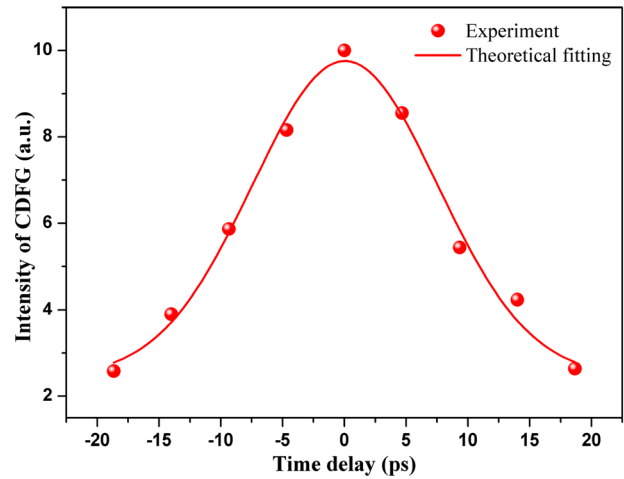


FIG. 4. Dependence of the cascaded CSHG intensity on the input power intensity of the pump at 532 nm.



(a)



(b)

FIG. 5. The intensity evolutions of spot ③ when moving the prism from  $+x$  axis to  $-x$  axis in steps of 0.7 mm (a). The dependence of the normalized CDFG intensities on time delay as well as the theoretical fitting (b).

shown in Fig. 4. From the figure, we can find that  $I_3$  increased with  $I_{532}$  and was fitted to be a linear relationship, which was in good agreement with the theoretical prediction.

To investigate the dependence of the radiation on the temporal overlapping of the two interacting pulses, we kept the energies of the two pulses at fixed values and scanned the prism from  $+x$  to  $-x$ . By moving the prism in steps of 0.7 mm, i.e., gradually increasing the optical path of the 532 nm light, the temporal overlapping between the two pulses was first increased and then reduced. From Fig. 5(a), we can see that the intensity of spot ③ first increased and then decreased. As discussed above, intensity  $I_3$  was proportional to  $I_{1064}^{CR}$ , which indicated that the variations trend of the CDFG intensity could be entirely represented by that of  $I_3$ . So we can get the normalized intensity of CDFG varying with the delay time, as shown in Fig. 5(b), which was in well accordance with theoretical fitting using Eq. (5).

In conclusion, we have achieved CDFG ( $\vec{k}_{532} - \vec{k}_{1064} \rightarrow \vec{k}_{1064}$ ) in a 2D rectangular PPLT crystal. Due to the participation of the backward reciprocal vector, the phase velocity of the NPW was accelerated to exceed the threshold for realizing CDFG. The Čerenkov angles of all the radiations and the intensity dependent properties of the interactions were discussed. In addition, we investigated the dependence of the intensity of CDFG on the time delay of the two pulses through a cascaded CSHG process. Our results indicate that such a scheme is an effective approach for realizing Čerenkov down-conversion, and related works such as Čerenkov optical parametric generation are under way.

This work was supported by the Jiangsu Science Foundation (BK2011545), the State Key Program for Basic Research of China (Nos. 2010CB630703 and 2011CBA00205), the

National Natural Science Foundations of China (Nos. 11004097 and 11021403). It was also supported by the Priority Academic Program Development of Jiangsu Higher Education Institutions (PAPD).

- <sup>1</sup>P. A. Čerenkov, Dokl. Akad. Nauk SSSR **2**, 451 (1934).
- <sup>2</sup>P. K. Tien, R. Ulrich, and R. J. Martin, *Appl. Phys. Lett.* **17**, 447 (1970).
- <sup>3</sup>K. Hayata, K. Yanagawa, and M. Koshiba, *Appl. Phys. Lett.* **56**, 206 (1990).
- <sup>4</sup>H. Tamada, *IEEE J. Quantum Electron.* **27**, 502 (1991).
- <sup>5</sup>N. A. Sanford and J. M. Connors, *J. Appl. Phys.* **65**, 1429 (1989).
- <sup>6</sup>K. Hayata and M. Koshiba, *J. Opt. Soc. Am. B* **8**, 449 (1991).
- <sup>7</sup>C. D. Chen, J. Su, Y. Zhang, P. Xu, X. P. Hu, G. Zhao, Y. H. Liu, X. J. Lv, and S. N. Zhu, *Appl. Phys. Lett.* **97**, 161112 (2010).
- <sup>8</sup>A. Fragemann, V. Pasiskevicius, and F. Laurell, *Appl. Phys. Lett.* **85**, 375 (2004).
- <sup>9</sup>Y. Sheng, S. M. Saltiel, W. Krolikowski, A. Arie, K. Koynov, and Y. S. Kivshar, *Opt. Lett.* **35**, 1317 (2010).
- <sup>10</sup>Y. Zhang, F. M. Wang, K. Geren, S. N. Zhu, and M. Xiao, *Opt. Lett.* **35**, 178 (2010).
- <sup>11</sup>P. Molina, M. O. Ramirez, B. J. Garcia, and L. E. Bausa, *Appl. Phys. Lett.* **96**, 261111 (2010).
- <sup>12</sup>K. Kalinowski, Q. Kong, V. Roppo, A. Arie, Y. Sheng, and W. Krolikowski, *Appl. Phys. Lett.* **99**, 181128 (2011).
- <sup>13</sup>W. J. Wang, Y. Sheng, Y. F. Kong, A. Arie, and W. Krolikowski, *Opt. Lett.* **35**, 3790 (2010).
- <sup>14</sup>H. J. Ren, X. W. Deng, Y. L. Zheng, N. An, and X. F. Chen, *Phys. Rev. Lett.* **108**, 223901 (2012).
- <sup>15</sup>H. X. Li, S. Y. Mu, P. Xu, M. L. Zhong, C. D. Chen, X. P. Hu, W. N. Cui, and S. N. Zhu, *Appl. Phys. Lett.* **100**, 101101 (2012).
- <sup>16</sup>M. Ayoub, P. Roedig, J. Imbrock, and C. Denz, *Appl. Phys. Lett.* **99**, 241109 (2011).
- <sup>17</sup>Y. Sheng, W. J. Wang, R. Shiloh, V. Roppo, Y. F. Kong, A. Arie, and W. Krolikowski, *Appl. Phys. Lett.* **98**, 241114 (2011).
- <sup>18</sup>N. An, H. J. Ren, Y. L. Zheng, X. W. Deng, and X. F. Chen, *Appl. Phys. Lett.* **100**, 221103 (2012).
- <sup>19</sup>Y. Zhang, Z. D. Gao, Z. Qi, S. N. Zhu, and N. B. Ming, *Phys. Rev. Lett.* **100**, 163904 (2008).
- <sup>20</sup>C. D. Chen, J. Lu, Y. H. Liu, X. P. Hu, L. N. Zhao, Y. Zhang, G. Zhao, Y. Yuan, and S. N. Zhu, *Opt. Lett.* **36**, 1227 (2011).